

Pixel Size Calibration of Video Probe Measuring Machines

James G. Salsbury

Center for Precision Metrology

University of North Carolina at Charlotte

Coordinate measuring machines (CMMs) equipped with video probing systems are becoming more and more popular for dimensional metrology in a variety of industries. The typical off-the-shelf machine being commonly implemented today utilizes a charge-coupled device (CCD) camera mounted to a two or three axis measuring machine frame. As with any type of measuring machine, there are calibration issues with the probing sensor. For a video probe measuring system, one of the key issues is the calibration of the actual magnification of the video system. This calibration process is usually referred to as the calibration of the pixel size, which is in reference to the use of a CCD camera with a particular array of pixels. The various magnification objectives (or zoom lens) will result in different amounts of the measured surface being mapped onto the pixel array. The pixel size calibration process is essentially the calibration of the video probe scale relative to a traceable length standard.

The most common method to calibrate the pixel size is to measure some type of artifact with calibrated features that fit completely inside the field of view of the video sensor for the particular magnification of interest. The ratio between the calibrated value of the feature and the number of measured pixels is used to calibrate the pixel size. Another less commonly used technique for pixel size calibration does not require an externally calibrated artifact but rather utilizes the scales of the measuring machine's own stage, i.e. a self-calibration technique.

In this paper the uncertainty of the process used to calibrate the pixel size is investigated. The effect of various types of calibration artifacts, such as chrome-on-glass circles, linewidths, and grid patterns are evaluated and contrasted. General equations are developed that allow the uncertainty of the pixel calibration process to be estimated for various types of machines and magnification levels. Experimental results are also presented.

Application and Assumptions

This paper is concerned with typical video probe measuring machines that are being implemented everyday in various industries. The application of these machines is to be considered general in nature. The calibration of the video probe is not considered to be specific to a particular measurement. If only a specific feature is to be measured with a machine of this class, then the calibration process should be developed to imitate the application in order to reduce the measurement uncertainty [1,2].

There are a large number of video probe CMM manufacturers; however, the vast majority of the machines, and the ones considered in this paper, fall into a class defined by a scale resolution of around 0.5 to 0.1 micrometers, a measuring field of view from 6 mm to 0.25 mm, and the use of a CCD camera with around 500-800 pixels linearly. These machines typically have a quoted accuracy in the neighborhood of 5 to 10 micrometers or less. Machine manufacturers handle the integration and calibration of the video probe in different manners. The analysis presented here will be kept general and will also only consider one axis for simplicity.

In estimating the measurement uncertainty, the approach of the ISO *Guide to the Expression of Uncertainty in Measurement* (GUM) [3] will be utilized. In this paper, a number of uncertainty sources will be considered negligible and others will be evaluated in specific manners based on convenience. The uncertainty of all the contributors will be estimated based on available data, experience, and knowledge, and will utilize the Type B evaluations allowed by the GUM. Specific uncertainty sources that will not be considered include distortion and illumination variation across the field of view and thermal effects.

Artifact Based Calibration

There are a variety of two-dimensional artifacts available that can be used for the pixel size calibration. The most common are chrome-on-glass where the features are circles, squares, grids, or lines. National labs such as NIST and PTB have programs for the calibration of some of these artifacts with uncertainties around 10 to 50 nm [1,4]. Various commercial calibration labs are also capable of calibrating these types of artifacts with uncertainties ranging from around 100 nm to 1 μm and up depending on capability and cost. When one of these types of artifacts is used

for the pixel size calibration, such as shown in Figures 1 and 2, the features to be measured need to be positioned completely inside the range, or the field of view, of the video probe sensor. With the initial pixel size set to some value, C_0 , the feature is measured, and the calibrated value, L_c , is compared to the measured value L_m . The calibrated pixel size, C , is therefore defined by

$$C = C_0 \frac{L_c}{L_m} \quad (1)$$

For the purposes of evaluating the uncertainty of the pixel size calibration, this equation is rewritten in terms of the number of measured pixels, N . Since $L_m = NC_0$, Eq. (1) can be reduced to

$$C = \frac{L_c}{N} \quad \text{where } L \text{ is used in place of } L_c. \quad (2)$$

In accordance to the GUM, the uncertainty of the pixel size, C , can be expressed as follows:

$$u_C^2 = \frac{C}{L}^2 u_L^2 + \frac{C}{N}^2 u_N^2 + 2 \frac{C}{L} \frac{C}{N} u_L u_N \quad (3)$$

Since L and N are independent of each other, Eq. (3) reduces to the following, with the appropriate sensitivity coefficients also included:

$$u_C^2 = \frac{1}{N^2} u_L^2 + \frac{L}{N}^2 u_N^2 \quad (4)$$

The uncertainty contributors, u_L and u_N , need to be estimated. Using a Type B evaluation, the uncertainty in the number of measured pixels, u_N , can be estimated for this class of machine using data and information from available literature [1,5,6,7,8]. Though there are a variety of error sources associated with using a video probe that might be included in the estimate of u_N , a detailed analysis of those sources is beyond the scope of this paper. Based on the available published data from the literature, the worst expected error is estimated to be 0.2 pixels. A Gaussian distribution for this uncertainty is assumed with the 95% limits being defined by ± 0.2 pixels. This results in

$$u_N = 0.1 \text{ pixels} \quad (5)$$

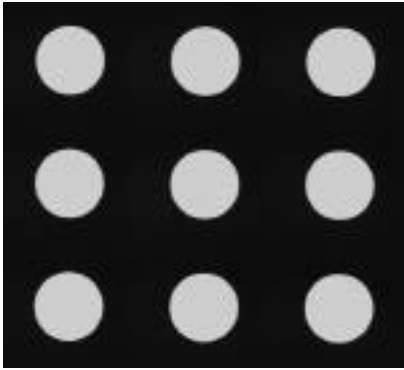


Figure 1: Circle artifact as seen by video probe.

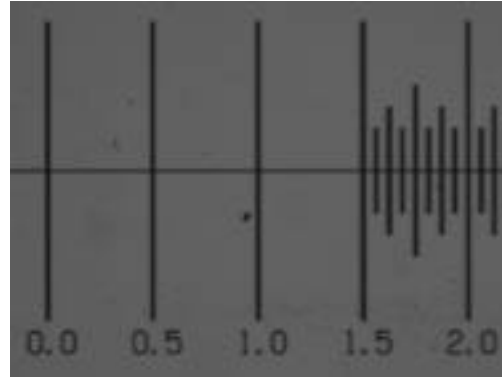


Figure 2: Line scale artifact as seen by video probe.

In this paper, two different types of artifacts are considered. The first type has the calibrated features being unidirectional in nature, such as distances between feature centers. The second has the calibrated features being bidirectional in nature, such as linewidths and circle diameters. Due to errors in edge finding, there is more uncertainty in the measurement of bidirectional features than unidirectional ones [1,5,6,7]. Since this bidirectional error will manifest itself in the measurement process as an increase or decrease in the size of the measured feature, the additional uncertainty due to using bidirectional features is combined into the uncertainty contributor u_L as

$$u_L^2 = u_a^2 + u_b^2 \quad (6)$$

where u_a is the estimated uncertainty of the calibrated value of the artifact and u_b is the additional uncertainty due to the use of a bidirectional artifact. Eq. (6) assumes independency with sensitivity coefficients of one. With a properly calibrated artifact, a Type B evaluation for the uncertainty estimate of u_a should be straightforward using the calibration certificate from the supplier. The estimate of u_b is more challenging; however, there are data available in the literature that can be used to make a Type B evaluation for this class of machine [5,6,7]. Based on the available data, plus additional data gathered on the machines under test, the maximum bidirectional error is estimated to be

approximately 0.35% of the field of view being used. For the purposes of this paper, the field of view is defined by a single number equal to the diameter, D , of the largest circle that can be circumscribed in the two-dimensional range of the video sensor when using a specific magnification. To estimate the standard uncertainty u_b , it is assumed that the bidirectional error follows a Gaussian distribution and that the maximum error defines the 95% limits of the distribution. The standard uncertainty can then be estimated by

$$u_b = \frac{0.0035}{2} D = 0.00175D \quad (7)$$

Eqs. (4) to (7) can be combined together to express the uncertainty of the artifact calibration approach, U_{AC} , using a coverage factor, $k = 2$, as

$$U_{AC} = \frac{2}{N} u_a^2 + \frac{0.1L}{N}^2 + (0.00175D)^2 \quad (8)$$

where D is defined as equal to zero if the measured features are unidirectional in nature.

Self-Calibration Approach

An external artifact is not necessary to calibrate the pixel size. It is possible, instead, to calibrate the pixel size using the scales of the machine stage. This process simply requires a small measurable feature to be fixed to the stage and then moved across the field of view. The location of the small feature is measured in two positions along with the distance the machine stage is moved. This technique has been shown to be easily feasible on all video probe CMMs tested to date. The process is shown pictorially in Figures 3 and 4. In Fig. 3, the location of the small circular feature is measured along with the coordinates of the cross-hair shown. The stage is then moved and the location of the circular feature and cross-hair are again measured as shown in Figure 4. The difference between the two measurements of the cross-hair, L , which is independent of the video probe, determines the distance moved by the stage. The difference between the two measurements of the circular feature, δ , which is nominally zero, represents an amount of error that is the resultant of any error in the initial calibration of the pixel size. The self-calibration approach can be represented by the following:

$$C = C_0 \frac{L}{L - \delta} \quad (9)$$

To estimate the uncertainty in the self-calibration of the pixel size, C , it is convenient to express δ in terms of the number of pixels, N , where $\delta = L - NC_0$. Eq. (9) can be shown to reduce to Eq. (2). Eqs. (2), (3), and (4) therefore apply to both the artifact and the self-calibration approaches, with the only difference being that L is defined as the length over which the self-calibration is done, instead of the length of the calibrated artifact feature.

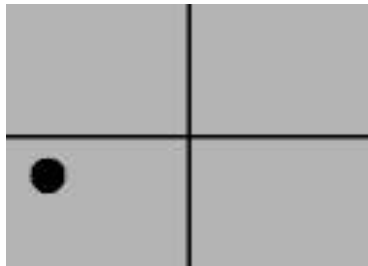


Figure 3: Self-calibration position one

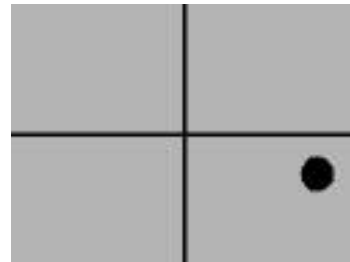


Figure 4: Self-calibration position two

As discussed previously for the artifact based approach, Eq. (5) also applies for the uncertainty of the pixel size, u_N , for the self-calibration approach. The uncertainty contributor, u_L , however, needs to be estimated. This is done by assuming that this uncertainty contributor can be estimated by two different uncertainty sources, u_{LDA} , the uncertainty due to linear displacement accuracy (or LDA) of the machine axis moved, and u_R , the uncertainty due to the apparent non-repeatability of the measuring system. Assuming that these contributors are independent with sensitivity coefficients equal to one, then u_L can be expressed as

$$u_L^2 = u_{LDA}^2 + u_R^2 \quad (10)$$

The uncertainty due to the apparent non-repeatability, u_R , is estimated with a Type B evaluation from machine specifications and from prior experience with the particular machines under test. In the context used here, u_R represents lack of repeatability in the machine stage and does not include effects of the video probe itself.

The estimation of the uncertainty due to the LDA is a bit more challenging. Well-accepted performance standards exist for calculating the LDA of measuring machines [9] and machine tools [10]. There are not, however, any generally accepted methodologies for reducing the LDA of a longer axis to generate uncertainty estimates over very short distances (where $L \ll$ full axis travel). A method is proposed here to estimate the maximum displacement error over a short distance by assuming some knowledge regarding the typical form of the error across the full travel of the axis. All the existing standards assume slowly spatially varying errors and have defaults for measurement points around every 25 mm or from 10% to 20% of the maximum traverse distance of the axes. From this information, the shortest likely wavelength of the displacement error, λ , is estimated; that assumption, along with an estimate of the maximum amplitude, A , is used to estimate the worse case displacement error over a much shorter distance, in particular, over the calibration length, L . The equation of the displacement error, δ , due to this shorter wavelength is defined by

$$\delta = A \sin \frac{2\pi}{\lambda} X \quad (11)$$

where X is the nominal motion of the machine axis. The maximum rate of change of this error is equal to the maximum slope of Eq. (11). Assuming that $L \ll \lambda$, then the error at the maximum slope is approximately linear over the distance L , and therefore the maximum error over the distance L can be approximated by the maximum slope multiplied by L . Assuming a triangular distribution for this uncertainty contributor with the higher and lower limits being equal to plus or minus the maximum error results in the following:

$$u_{LDA} = 2.5 \frac{AL}{\lambda} \quad (12)$$

Eq.(12) is combined with Eqs. (10), (5), and (4) to express the uncertainty of the self-calibration approach. Applying a coverage factor, $k=2$, results in

$$U_{sc} = \frac{2}{N} u_R^2 + \frac{2.5AL}{\lambda}^2 + \frac{0.1L}{N}^2 \sqrt{2} \quad (13)$$

Experimental Results

Experimental tests were done on a View Voyager and a Werth Inspector, two different video probe CMMs located in the Center for Precision Metrology at UNC Charlotte. The View has 0.1 μm scales and is a larger floor mounted machine; the Werth has 0.5 μm scales and is a smaller bench-top machine. Tests were done on both machines using the same 2X ($D=3$ mm, $NA=0.055$) and 20X ($D=0.3$ mm, $NA=0.42$) plan apochromat objectives from Mitutoyo. In reference to Eqs. (13) and (8), the estimates for the View machine are $u_R = 200$ nm and $A = 2000$ nm. For the Werth, the estimates are $u_R = 300$ nm and $A = 3000$ nm. For both machines, λ was estimated at 25 mm. The values for the remaining variables, u_a , N , and L , were determined from the specific artifact and sensor range used.

For each machine at each magnification, the pixel size was calibrated using three trials of six different methods, for a total of 72 different calibrations under various conditions. Of the six methods, two utilized unidirectional artifacts, two utilized bidirectional artifacts, and two utilized the self-calibration approach. The results for the Werth machine tests with the 20X objective are shown in Fig. 5. The pixel size deviation in the plot is determined by subtracting the pixel size of each calibration from the average of the three calibrations of the method with the lowest estimated uncertainty (trials 13-15 in this case). The plot shows both the calibration results and the estimated uncertainty. Trials 1-3 were done with an unidirectional circle artifact (see Fig. 1), trials 4-6 were done using the self-calibration technique, trials 7-9 and 10-12 were done with two different bidirectional circle diameter artifacts, trials 13-15 were done with a line scale calibrated at NIST (see Fig. 2), and trials 16-18 were done using the self-calibration technique using an average of nine independent trials.

To compare all 72 results with each other, the deviation of each was divided by its estimated uncertainty. These results are shown in Fig. 6. If the uncertainties were estimated well, then approximately 95% of the data would fall between ± 1 in this plot. As can be seen in the plot, six points lie outside this band, which results in 91.7% of the points being inside. Three of the points are very near to being inside the band; if they are considered in, then the percentage increases to 95.8%. In addition, the standard deviation of the data shown in Fig. 6 is approximately equal to the ideal value of 0.5. Based on this limited sample size, the models used to estimate the measurement uncertainty seem to work well. In addition, the estimated uncertainties of the self-calibration techniques are less than the uncertainties of the calibrations with the bidirectional artifacts and are close in magnitude to the unidirectional tests.

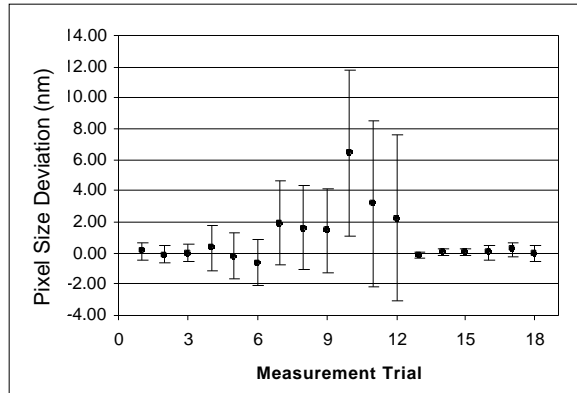


Figure 5: Werth 20X results and uncertainty

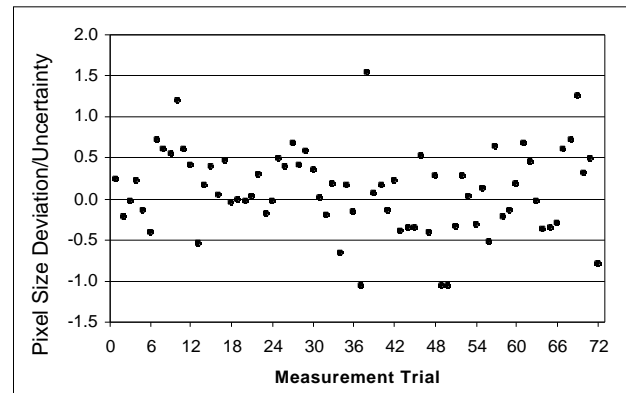


Figure 6: All results, expressed as (Deviation/Uncertainty)

These results indicate that the use of artifacts for pixel size calibration may be unnecessary except in cases where extremely high magnification and accuracy is needed or where the quality of the machine scale is poor. In this work, only the trials that were done with a NIST calibrated line scale, with a standard uncertainty of 10 nm, gave significant improvements over the self-calibration approach. For the class of machines considered in this work, extremely high magnification objectives are not common (rarely 50X or higher), and the machines will most likely have adequate scale accuracy for use with the self-calibration approach.

Acknowledgments

This work was made possible through the support of the National Science Foundation I/UCRC program and all the affiliate members of the Center for Precision Metrology at UNC Charlotte. In particular, the author would like to acknowledge the support of GSI-Lumonics (View Engineering). The author would also like to thank Scott Schmidt at Siecor Corporation and Art Whistler at Werth America for the use of artifacts that were critical to the experimental studies and Dr. Robert Hocken at UNC Charlotte for his review of this work.

References

1. Vezzetti, C., Varner, R. N., and Potzick, J. E., *Bright-Chromium Linewidth Standard, SRM 476, for Calibration of Optical Microscope Linewidth Measuring Systems*, NIST special publication 260-114, National Institute of Standards and Technology, Gaithersburg, MD, January 1991.
2. Hunsicker, R. J., Patten, J., Ledfort, A., Ferman, C., and Allen, M., "Automatic Vision Inspection and Measurement System for External Screw Threads," *Journal of Manufacturing Systems*, 13(5), 1994.
3. *Guide to the Expression of Uncertainty in Measurement*, International Organization for Standardization, Geneva, Switzerland, 1995.
4. Ha ler-Grohne, W., and Bosse, H., "Characterization of the long-term reproducibility of 2D coordinate photomask calibration at the PTB", *Proceedings of the 1st International Conference of the European Society for Precision Engineering and Nanotechnology*, Bremen, 1999.
5. De Chiffre, L., and Hansen, H. N., "Metrological Limitations of Optical Probing Techniques for Dimensional Measurements," *Annals of CIRP*, 44(1), 1995.
6. Thakkar, H. H., *Characterization of Hybrid Coordinate Measuring Machines*, UNC Charlotte Master's Thesis, 1998.
7. Garces, A., Huser-Teuchert, D., Pfeifer, T., Scharsich, P., Torres-Leza, F., and Trapet, E., *Performance Test Procedures for Optical Coordinate Measuring Probes*, Report on contract no. 3319/1/0/159/89/8-BCR-D(30), European Communities, Brussels, 1993.
8. Kim, S., "Measurement Uncertainty Limit of a Video Probe in Coordinate Metrology," *Annals of CIRP*, 45(1), 1996.
9. ASME B89.4.1-1997, *Methods for Performance Evaluation of Coordinate Measuring Machines*, American Society of Mechanical Engineers, New York, NY, 1997.
10. ASME B5.54-1992 (R1998), *Methods for Performance Evaluation of Computer Numerically Controlled Machining Centers*, American Society of Mechanical Engineers, New York, NY, 1998.